AN EXPERIMENTAL AND COMPUTATIONAL ANALYSIS OF BUOYANCY DRIVEN FLOWS BY LASER SHEET TOMOGRAPHY, PARTICLE IMAGE VELOCIMETRY AND COMPUTATIONAL FLUID DYNAMICS

MT Stickland, TJ Scanlon, A Oldroyd, P Waddell
Department of Mechanical Engineering,
University of Strathclyde,
Glasgow,
Scotland

F Crawley, B Stubbs
Department of Chemical and Process Engineering,
University of Strathclyde,
Glasgow,
Scotland

ABSTRACT

This paper contains details of a three pronged investigation into the development of a buoyant jet impinging on a wall in a closed vessel. The development of the flow was measured experimentally by particle image velocimetry (PIV) and laser sheet tomography. The experimental results are compared with a computational model of the flow calculated by the computational fluid dynamics (CFD) package PHOENICS.

NOMENCLATURE

g	accelaration due to gravity
p	pressure
t	time
u	x - velocity component
v	y - velocity component
C	Species concentration
C_{inc}	Species concentration of incoming fluid
C_{rec}	Species concentration of receiving fluid
CFD	Computational Fluid Dynamics
PIV	Particle image velocimtery
S_u	Source of momentum in the x direction
S_v	Source of momentum in the y direction
S_C	Source of species concentraton
TIF	Tagged Image Foramt
ρ	density
ρ_{inc}	density of the incoming fluid
ρ_{rec}	density of the receiving fluid
μ_λ	laminar dynamic viscosity
μ_τ	turbulent dynamic viscosity
σ_λ	laminar Prandtl Number
σ_τ	turbulent Prandtl Number
$\Gamma_{\varepsilon\phi\phi}$	Diffusion Coefficient

INTRODUCTION

The Piper Alpha disaster in the British North Sea in 1988 was a horrific example of the dangers of a gas build up within a confined space. This accident claimed the lives of 167 people including two of the rescue workers [1]. Whilst this scale of accident is fortunately rare, confined leaks which may lead to an explosion are not uncommon within industry. Gas leaks in the domestic environment may also have tragic consequences. Flammable gas leaks may cause explosions and fires whilst faulty domestic heaters may cause death by carbon monoxide inhalation This paper will detail the experimental techniques required for an investigation into how these confined gas leaks may be modeled by sub scale experiments using water and brine to simulate buoyant gases in air. A simplified system of a jet of fluid impinging on a wall is initially assessed. The results of the experimental work are compared to a computational fluid dynamics (CFD) model.

The advent of the powerful, desktop, personal computer in the 1980s has led to computational fluid dynamics becoming an important analytical tool for engineers. This paper uses CFD to analyse the behaviour of a jet of fluid issuing into an enclosed space containing a fluid of higher density. The effects of the buoyancy, diffusion and momentum of the jet on its dispersion within the enclosed space are studied.

The results of the CFD model are compared with an experimental model. The dispersion of salt and sugar solutions in fresh water within the enclosed space of the experimental model is studied by laser tomography and particle image velocimetry (PIV).

EXPERIMENTAL TECHNIQUES

Particle Image Velocimetry

Particle image velocimetry is, now, a common technique which allows the whole flow field's velocity to be mapped instantaneously by computationally analysing a picture of the flowfield. This image has multiple exposures of the flow which has been seeded with small particles and illuminated by a thin sheet of laser light. PIV has been applied to numerous flows ranging from low speed bluff body flows [2], high speed flows

[3], combusting flows [4], two phase flows [5] and turbomachinery [6]. The technique is now an established tool within the experimental fluid mechanics community and will not, therefore be described in detail within this paper. For information on PIV in general the reader is recommended to consult [7].

The laser sheet was produced by a 5W Spectra Physics 165 Argon Ion laser and cylindrical lens. Typically only 2.5W of laser power were required for imaging purposes. Modulation of the laser beam was by a mechanical beam chopper consisting of a circular disk with 90 slots on its perimeter turned by a variable speed DC motor. Measurement of the modulation frequency was by a fibreoptic-photodiode arrangement. The fibreoptic cable and lens was placed such that reflected light from the acrylic casing was sufficient to switch the photodiode. The system was simple and reliable. A diagram of the experimental setup and the frequency measuring photodiode circuit diagram are shown in figure 1. The fibre optic cable and lens were salvaged from a laser printer. Images were acquired by a Sony XC75 768 x 494 pixel monochrome CCD camera connected to a Matrox frame grabber card in a 486SX25 PC. The images were analysed by Optical Flow Systems VidPiv PIV analysis Software by autocorrelation on a 486DX266 PC

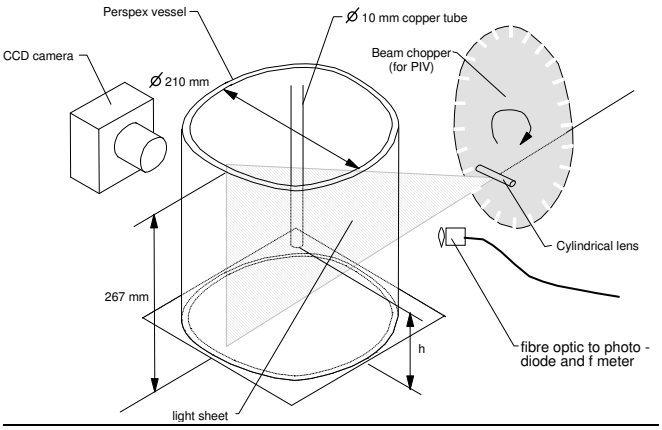

Figure 1. Experimental apparatues

Laser Tomography

Laser tomography images are obtained by illuminating the flow field with a sheet of light. This illuminates the fluid jet which has been seeded by a fine powder (milk powder) or dye . The intensity of the reflected light is proportional to the concentration of the seeding particles in the jet and hence to the concentration of the fluid solution in the jet. As the jet diffuses into the transparent fluid enclosed within the vessel the concentration of the seeding particles in the jet decreases and hence the intensity of the scattered light is reduced. The images of the flow are grabbed by a CCD camera and the monochrome image produced is processed to produce a false colour representation of the concentration distribution within the jet. The false colour image is then easily compared with the graphical output of the CFD program.

The light intensity within the captured image is stored in a TIF file as eight bit data representing 256 levels of gray from white (gray scale 0) to black (grayscale 255). To each gray scale is assigned a false colour so that a spectrum of colours is obtained, each corresponding to a different gray scale and hence concentration, figure 2.

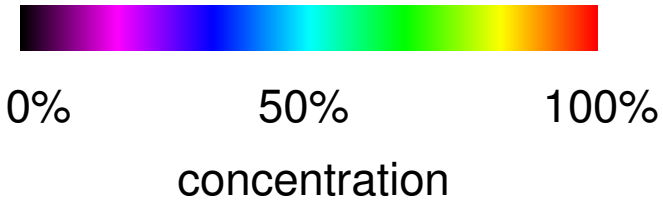

Figure 2. Calibration colour chart

The TIF file is then processed by the false colour program and the gray scales changed to produce a false colour representation of the flow, figure 3.

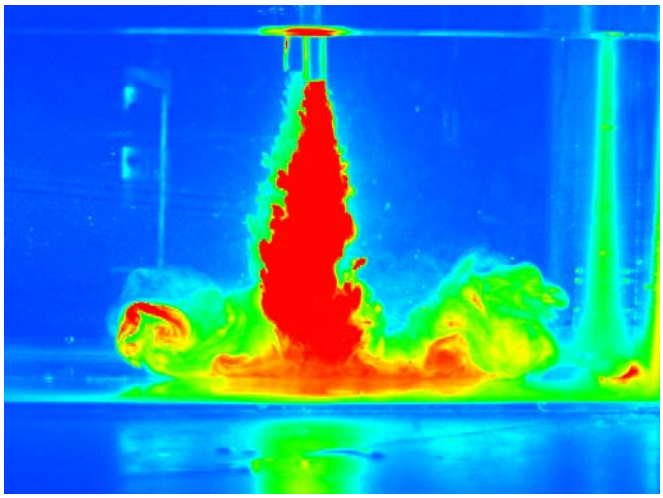

Figure 3. False colour image

Because we wish to extract quantitative data from these false colour images care must be taken to calibrate the optics before images are acquired. Initially, for a fixed illumination level and aperture setting the concentration of seeding powder required to produce 0 grayscale is determined. This is defined as 100% concentration. If too high a seeding concentration is allowed in the jet then saturation of the image may occur as shown in figure 4.

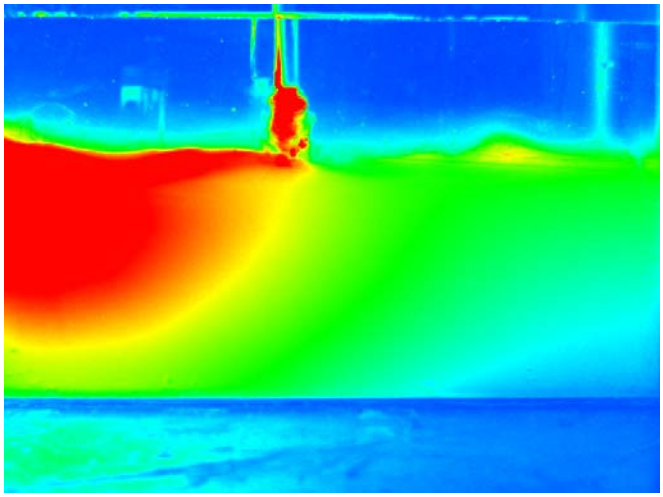

Figure 4. Effect of high seeding concentration

In this image we see that the symmetric distribution of concentration within the vessel is not achieved and a high concentration level is found to the left. This is due to the high seeding level attenuating the light sheet producing uneven illumination and hence indicating a lower concentration in the shadowed region to the right.

NUMERICAL MODEL

The work in this paper has been carried out within the framework of the general purpose commercial CFD (Computational Fluid Dynamics) code PHOENICS [8].

Geometrical Configuration

The geometry has been generated within a two-dimensional polar-cylindrical coordinate system $(Y,Z) \rightarrow (r,z)$. A computational mesh of 55Y by 70Z was employed as shown in figure 5. A transient analysis was considered with solutions achieved at various time intervals over a total period of 30 seconds.

Governing Equations

The fluid flow was modeled by partial differential equations describing the conservation of mass, momentum and species concentration for unsteady, incompressible flow:

conservation of mass

$$\nabla . \boldsymbol{u} = 0 \qquad \text{...(1)}$$

conservation of momentum

$$\rho \frac{\partial \boldsymbol{u}}{\partial t} + \rho \nabla . (\boldsymbol{u} \otimes \boldsymbol{u}) = -\nabla p + \nabla . (\Gamma_{\text{eff}} \nabla \boldsymbol{u}) + \rho \mathbf{g} + \mathrm{S}_{\boldsymbol{u}} \qquad \text{...(2)}$$

conservation of species concentration

$$\rho \frac{\partial C}{\partial t} + \rho \nabla . (\boldsymbol{u} C) = \nabla . (\Gamma_{\text{eff}} \nabla C) + \mathrm{S}_C \qquad \text{...(3)}$$

where

$$\Gamma_{\text{eff}} = \left(\frac{\mu_{\text{l}}}{\sigma_{\text{l}}} + \frac{\mu_{\text{t}}}{\sigma_{\text{t}}} \right) \qquad \text{...(4)}$$

Slight changes in the density of the incoming (subscript *inc*) and receiving (subscript *rec*) fluids may be taken into account by assuming a simple linear variation in density with the local concentration of incoming fluid, such that:

$$\rho_{actual} = \rho_{inc} C_{inc} + \rho_{rec} C_{rec} \qquad \text{...(5)}$$

where

$$C_{inc} = 1.0 - C_{rec} \qquad \text{...(6)}$$

The standard form of the well known 2-equation $k - \varepsilon$ turbulence model was also implemented for turbulence closure.

Solution algorithm

In the numerical model a control volume/finite difference formulation is used. The above equations are integrated over each control volume to obtain a set of discretised linear algebraic equations of the form:

$$a_P \phi_P = \sum a_{nb} \phi_{nb} + b \qquad \text{...(7)}$$

Equations of the type (7) are called finite volume equations and equation (7) describes the transient, convective and diffusive processes affecting the value of ϕ in cell P in relation to its neighbouring cells (subscript *nb*) and source term *b*. These equations were solved using an iterative solution process based on the SIMPLEST [9] algorithm. A staggered grid arrangement was employed for the discretisation of the momentum equations . For the discretisation of convective transport the HYBRID [10] scheme is the default scheme within the PHOENICS code. Implicit temporal differencing was chosen for the transient terms.

Boundary conditions

All boundary conditions were implemented by the inclusion of additional source and/or sink terms in the finite volume equations for the computational cells at the domain boundaries. No-slip conditions were applied at solid regions, these being the confining walls and pipe wall. An attempt was made to reduce the influence of the free surface boundary condition by positioning this boundary far from the domain of influence. Constant pressure was applied at the outlet surface.

Convergence criteria

An examination of the sum of the residual errors within each time-step for each of the equation sets solved gave an indication of the degree of convergence.

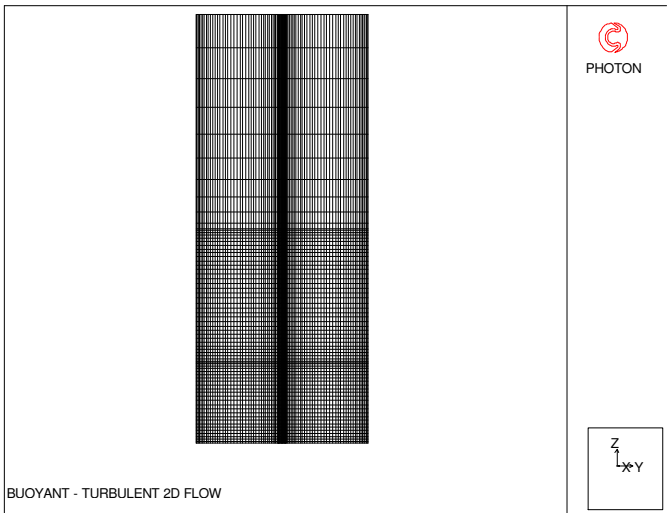

Figure 5. Computational grid

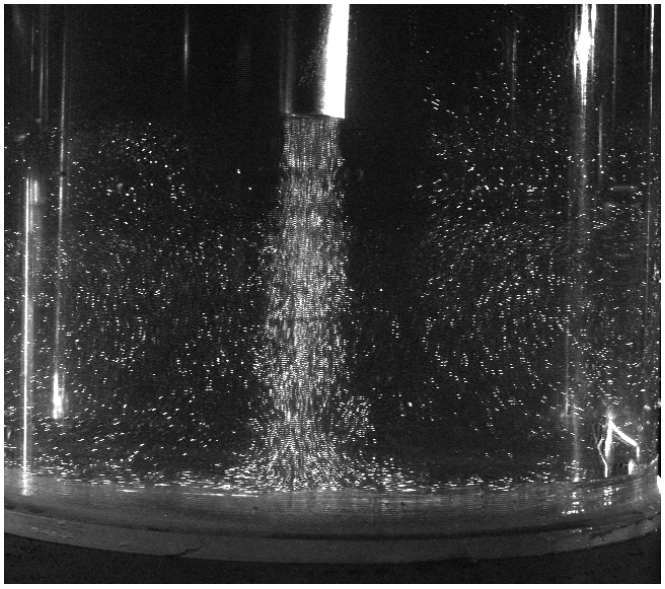

Figure 6. PIV image

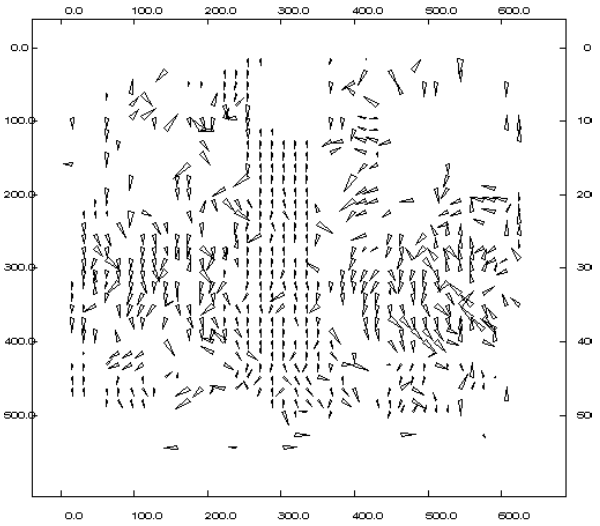

Figure 7. Vector map

DISCUSSION

It is interesting to compare the output of the CFD model with the experimental data obtained by PIV and laser tomography. All images shown below are of the jet after eight seconds into the transient. Figure 6 shows the raw PIV image for the flow, figure 7 shows the vector map found by an autocorrelation analysis of figure 6, figure 8 is a laser sheet tomography image of the flow field which has been processed to produce a false colour image of the flow. The concentration of seeding may be found in the calibration bar to the right of figure 8. Figure 9 is a plot of the CFD solution of the species concentration within the flowfield after the same time period

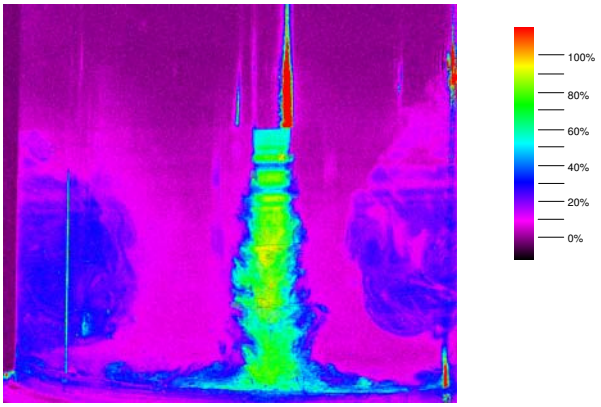

Figure 8. False colour image with calibration bar

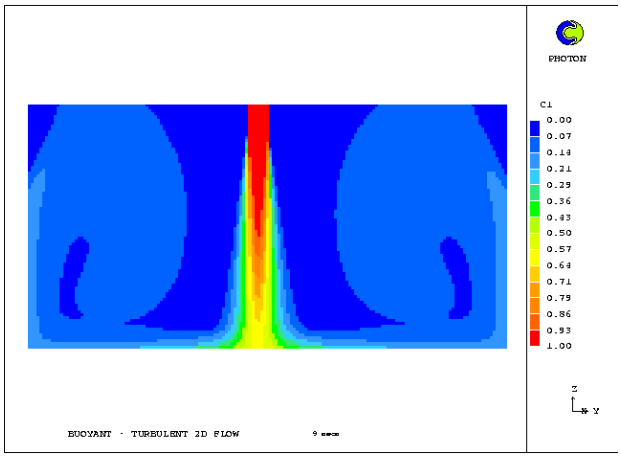

Figure 9. CFD model of flow

All image shown above are for the datum case of ordinary tap water flowing into a vessel containing ordinary tap water with a head of 5 cm between the reservoir and the cylindrical tank; Ra=0, Re=10,000. Several images were acquired for each transient; after one second and then at intervals of seven seconds.

It may be seen from the PIV image, figure 6, that the jet has impinged on the bottom of the vessel and reflected off the bottom and sides to form a characteristic "fountain flow" with two recirculation regions on the left and right of the image. Due to the curvature of the vessel data from the sides are not shown. The multiple illuminations of the particles as the image was acquired may be seen quite clearly. The flow was illuminated at a frequency of 1180 Hz with a laser power of 2.5 W exposure time of 1/250th and f8. This image was processed by autocorrelation to produce the vector map shown in figure 7. The magnitude of the velocity vectors calculated by CFDin the jet were within 10% of the experimental data.

The jet was also seeded with a small amount of milk powder to produce a slightly opaque solution to allow laser tomography. When seeded the laser power was reduced to 80mW and the aperture on the CCD set to f4 to produce sufficient reflected light. An image of the pure seeded liquid was acquired to obtain a 100% concentration calibration. The vessel filled with pure tap water was also imaged to obtain a 0% concentration calibration. The header tank was filled with 100% liquid and allowed to flow through the pipe into the vessel.

It may be seen from figure 8 that the core of the jet has a concentration of 90 to 100% for approximately seven pipe diameters (internal) downstream of the exit plane. The final three diameters before the jet impinges has a concentration of approximately 70%. Impingement causes rapid dispersion of the jet and creates a fountain flow with a concentration of 20%. The recirculation regions are quite distinct and the majority of the fluid remains pure tap water.

Comparison with the CFD output for this time during the transient shows that the concentration within the jet remains in the range 90-100% for approximately 8 diameters downstream of the exit lane. At impingement, the concentration is approximately 60% and the concentration within the dispersed jet is between 15% and 20%

It may therefore be seen that the CFD model of the flow provides quite good agreement with the laser tomography image of the flow field.

There is however some disagreement in the fine structure of the jet. It may be seen from figure 8 that the laser tomography image of the jet highlights the turbulent boundary of the jet whereas the CFD image is devoid of this structure. CFD is unable to model this phenomena of the flow and relies on the k-ε turbulence model to simulate this mixing process. The processes within this mixing layer have been extensively studied by Yule [11].

Due to the requirement for colour images to fully appreciate the techniques outlined in this paper it will also be published on the Mechanical Engineering WWW page at Strathclyde.

http://www.strath.ac.uk/Departments/MechEng/

CONCLUSIONS

It has been demonstrated that, with the use of PIV and laser tomography the flow vectors and concentration within an impinging jet may be found. The quantitative data obtained shows good agreement with the CFD model of the flow.

REFERENCES

(1) CULLEN, W.D. "The Public Enquiry Into The Piper Alpha Disaster" Department of Energy Report, HMSO October 1990

(2) BRUCE, T., EASSON, W.J., GREATED C.A. 'The kinematics of oscillatory flow past cylindrical structures' Proc. 3rd Int. Offshore and Polar Engineering Conference, Singapore, 1993

(3) KOMPENHANS, J., HOCKER, R., 'Application of Particle Image Velocimetry to High Speed Flow'. Lecture Series on Particle Image Displacement Velocimetry, Von Karman Institute for Fluid Dynamics, Belgium.

(4) REUSS, D.L., ADRIAN, R.J., LANDRETH, C.C., FRENCH, D.T., FANSHER, T.D. 'Instantaneous flames measurement of velocity and large scale vorticity and strain rate in and engine using particle image velocimetry' SAE Paper 890616, 1989

(5) HIND, A.K., McCLUSKEY, D.R., CHRISTY, J.R., EASSON, W.J., GREATED, C.A., GLASS, D.H. 'PIV analysis of two phase air-particle flows' IMechE symposium on Optical Methods and Data Processing in Heat and Fluid Flow, City University, London

(6) SHEPHERD, I.C., LAFONTAINE, R.F., 'Mapping the velocity field in a centrifugal fan using particle image velocimetry' Journal of Wind Engineering and Industrial Aerodynamics, 50 (1993) 373-382

(7) GRAY, C. 'The evolution of Particle Image Velocimetry,, IMechE Symposium On Optical Methods and Data Processing In Heat and Fluid Flow, City University, London 1992

(8) SPALDING, D.B. *"PHOENICS* ". CHAM TR/100, 1989.

(9) SPALDING, D.B. "Four Lectures on the PHOENICS computer code". Report CFD/82/S, Imperial College, London, 1982.

(10) PATANKAR, S.V. "Numerical Heat Transfer and Fluid Flow",(Hemisphere, New York), 1980.

(11) YULE, A.J. "Large Scale Structure In The Mixing Layer Of A Round Jet". Annual Review Of Fluid Mechanics, 14 (1982) 189-212